The Astrophysical Journal, 705:1548–1553, 2009 November 10 doi:10.1088/0004-637X/705/2/1548

A TRIGONOMETRIC PARALLAX OF Sgr B2

M. J. Reid[1], K. M. Menten[2], X. W. Zheng[3], A. Brunthaler[2], and Y. Xu[4]
[1] Harvard-Smithsonian Center for Astrophysics, 60 Garden Street, Cambridge, MA 02138, USA
[2] Max-Planck-Institut für Radioastronomie, Auf dem Hügel 69, 53121 Bonn, Germany
[3] Department of Astronomy, Nanjing University, Nanjing 210093, China
[4] Purple Mountain Observatory, Chinese Academy of Sciences, Nanjing 210008, China
Received 2009 August 25; accepted 2009 September 16; published 2009 October 23

ABSTRACT

We have measured the positions of H_2O masers in Sgr B2, a massive star-forming region in the Galactic center, relative to an extragalactic radio source with the Very Long Baseline Array. The positions measured at 12 epochs over a time span of one year yield the trigonometric parallax of Sgr B2 and hence a distance to the Galactic center of $R_0 = 7.9^{+0.8}_{-0.7}$ kpc. The proper motion of Sgr B2 relative to Sgr A* suggests that Sgr B2 is ≈ 0.13 kpc nearer than the Galactic center, assuming a low-eccentricity Galactic orbit.

Key words: astrometry – Galaxy: fundamental parameters – Galaxy: halo – Galaxy: kinematics and dynamics – Galaxy: structure – stars: formation

Online-only material: color figures

1. INTRODUCTION

Since the distance to the Galactic center (R_0) was first estimated by Shapley (1918), astronomers have expended considerable effort to measure R_0 accurately, and for good reason. All kinematic distances are proportional to R_0, and hence masses and luminosities of giant molecular clouds and their stars often depend directly on R_0. Most luminosity and many mass estimates (e.g., based on column densities) scale as the square of the source distance, while masses based on total densities or orbit fitting (using proper motions) scale as the cube of distance. For example, the estimate of the mass of the super-massive black hole at the Galactic center (Sgr A*) obtained from stellar orbits is dominated by uncertainty in R_0 (Ghez et al. 2008; Gillessen et al. 2009).

An accurate value for R_0 can also have significant impact in cosmology. Estimates of R_0 and Θ_0, the circular rotation speed of the Galaxy, are highly correlated. For example, measurement of the *apparent* secular motion of Sgr A* (Reid & Brunthaler 2004), caused by the orbit of the Sun around the Galaxy, yields the ratio Θ_0/R_0 directly. Thus, an accurate measurement of R_0, will give a correspondingly accurate estimate of Θ_0. The value of Θ_0 is critical for estimating the dark matter content of the Milky Way, to determine if the Large Magellanic Cloud (LMC) is bound to the Milky Way (Shattow & Loeb 2008), and, by changing the Andromeda infall speed, the total mass in the Local Group (Oort & Plaut 1975; Trimble 1986).

The value of the Hubble constant, H_0, is the single most important parameter for determining the age and size of the universe and, with cosmic microwave background fluctuations, the amount of dark matter and the equation of state of dark energy. Currently, H_0 is estimated to be 72 ± 3 (statistical) $\pm$ 7 (systematic) km s^{-1} Mpc^{-1} (Freedman et al. 2001). The $\approx$10% systematic uncertainty can be traced to the uncertainty in the assumed distance to the LMC. The accurate maser distance to NGC 4258, currently uncertain by $\pm$7% (Herrnstein et al. 1999), coupled with *Hubble Space Telescope* (*HST*) observations of Cepheids in that galaxy (Macri et al. 2006), provides a second anchor for the extragalactic distance scale and reduces the systematic error in H_0. An accurate distance to the Galactic center could add a valuable third anchor for the extragalactic distance scale. By measuring R_0 directly and with high accuracy, the spatial distributions of stars such as Cepheids could be used to re-calibrate the zero point of their period–luminosity relation, the reverse of the standard procedure where their magnitudes are assumed, and their distributions used to determine R_0 (Reid 1993), and hence reinforce the foundations of the extragalactic distance scale.

Measurement of R_0 is also important to the observational study of strong gravitational fields. Timing observations of the binary pulsar 1913+16 have placed important limits on gravitational waves. Damour & Taylor (1991) find that the largest uncertainty in modeling the orbital change of the binary comes from the acceleration of the Sun in its orbit about the center of the Galaxy (i.e., $\Theta_0{}^2/R_0$). Thus, improvement in our knowledge of the fundamental parameters of the Milky Way is crucial to improve the accuracy of important tests of strong gravitational fields.

R_0 has been estimated to be 8.0 ± 0.5 kpc ($\approx$6% accuracy) from an ensemble of classical techniques summarized by Reid (1993). Since then, many more measurements of R_0 using these techniques have been published, spanning the range 7.2 (Bica et al. 2006) to 8.7 kpc (Vanhollebeke et al. 2009). Most classical techniques involve determining the distributions of large numbers of bright sources that are assumed to be symmetrically distributed about the Galactic center. Distances to these sources are mostly photometric, which require accurate knowledge of absolute magnitudes and detailed calibration of the effects of metallicity, extinction, and crowding, and combined systematic uncertainties arguably are at least 5% and possibly larger.

Significant improvement in measuring R_0 is likely to come from techniques that are relatively direct. For example, measurement of stellar orbits in the Galactic center are not affected by most of the above mentioned systematic errors (but are sensitive to stellar crowding problems) and have yielded estimates of R_0 between 8.0 and 8.4 kpc, with uncertainties of about 0.4 kpc (Ghez et al. 2008; Gillessen et al. 2009). However, the most straightforward and direct technique for measuring distance in astronomy is trigonometric parallax. Parallaxes with accuracies

Table 1
VLBA Observations

Program	Date	Antennas Available									
		BR	FD	HN	KP	LA	MK	NL	OV	PT	SC
BR121A...	2006 Sep 4	√	√	√	√	√	√	√	√	√	√
BR121B...	2006 Sep 23	√	√		√	√	√	√	√	√	√
BR121C...	2006 Oct 9	√	√	√	√	√	√	√	√	√	√
BR121D...	2006 Oct 24	√	√	√	√	√	√	√	√	√	
BR121E...	2007 Mar 10	√	√		√	√	√	√	√	√	√
BR121F...	2007 Mar 17	√	√		√	√	√	√	√	√	√
BR121G...	2007 Mar 25	√	√	√	√	√	√	√		√	√
BR121H...	2007 Apr 4	√	√	√	√	√	√	√	√	√	√
BR121I.....	2007 Apr 22	√	√	√	√	√	√	√	√	√	√
BR121M...	2007 Sep 28	√		√	√	√	√	√	√	√	
BR121K...	2007 Sep 30	√	√	√	√	√	√	√	√	√	
BR121N...	2007 Oct 16	√	√	√	√	√	√	√	√	√	

Notes. Check marks indicate that antenna produced good data, while a blank indicates that little or no useful data were obtained. Antenna codes are BR: Brewster, WA; FD: Fort Davis, TX; HN: Hancock, NH; KP: Kitt Peak, AZ; LA: Los Alamos, NM; MK: Mauna Kea, HI; NL: North Liberty, IA; OV: Owens Valley, CA; PT: Pie Town, NM; and SC: Saint Croix, VI. Note that epoch M preceded epoch K as indicated. Ultimately, owing to scatter broadening of the image of J1745−2820, interferometer baselines longer than 2000 km could not be effectively used, limiting the usefulness of the HN, MK, and SC antennas for this study.

better than ±10 μas have recently been obtained with Very Long Baseline Interferometric (VLBI) techniques (Xu et al. 2006; Honma et al. 2007; Hachisuka et al. 2009; Reid et al. 2009a), and modeling the Galaxy with the full phase-space information provided by these observations holds great promise to determine R_0 and Θ_0 (Reid et al. 2009b).

We are now in a position to measure the distance to the Galactic center by trigonometric parallax. In this paper, we present the results of one year's observations with the National Radio Astronomy Observatory's[5] Very Long Baseline Array (VLBA) of H_2O masers in Sagittarius B2 (Sgr B2), the dominant high-mass star-forming region near the Galactic center (Snyder et al. 1994; Belloche et al. 2008). Sgr B2 contains several clusters of active star formation and we observed two of them, Sgr B2M and Sgr B2N. Each cluster displays ∼50 H_2O masers features spread over a region of size ∼2″ (Elmegreen et al. 1980; McGrath et al. 2004). Our VLBA data yield the first trigonometric parallax for the Galactic center. The measurement uncertainty from only one year's data is ±10%, demonstrating the promise of better accuracy with continued observation.

2. OBSERVATIONS AND DATA ANALYSIS

Our observations were conducted under VLBA program BR121. We observed Sgr B2M and Sgr B2N over 8 hr tracks at 12 epochs that spanned about one year (see Table 1 for details). The observing dates were chosen to sample only the peaks of the sinusoidal trigonometric parallax signature in right ascension, since the declination parallax amplitude is only ≈10% as great. This sampling provides maximum sensitivity for parallax detection and ensures that we can separate the secular proper motion (caused by projections of Galactic rotation, as well as any peculiar motion of the masers and the Sun) from the sinusoidal parallax effect.

[5] The National Radio Astronomy Observatory is a facility of the National Science Foundation operated under cooperative agreement by Associated Universities, Inc.

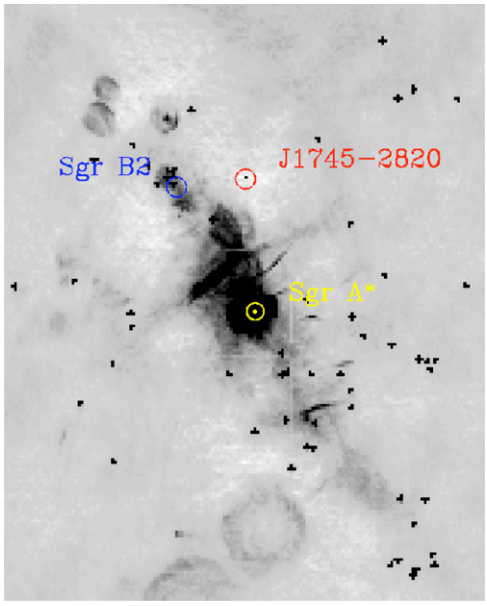

Figure 1. VLA 90 cm wavelength image, adapted from LaRosa et al. (2000), with the locations of Sgr A*, Sgr B2, and J1745−2820 indicated. The separation between Sgr B2 and J1745−2820 is ≈20′.

(A color version of this figure is available in the online journal.)

Table 2
Source Characteristics

Source	R.A. (J2000) (h m s)	Decl. (J2000) (d ′ ″)	θ_{sep} (deg)	P.A. (deg)	S_ν (Jy)	v_{LSR} (km s^{-1})
Sgr B2M...	17 47 20.150	−28 23 04.03	···	···	40	66.4
J1745−2820...	17 45 52.4968	−28 20 26.294	0.32	−82	0.1	···
Sgr B2N...	17 47 19.926	−28 22 19.37	···	···	13	56.7
J1745−2820...	17 45 52.4968	−28 20 26.294	0.32	−84	0.1	···

Notes. Coordinates are those used in the VLBA correlator. The position of J1745−2820 is accurate to about ±10 mas (Reid & Brunthaler 2004). Maser spots in both source are spread over a region of several arcseconds. Angular offsets (θ_{sep}) and position angles (P.A.) east of north of the background source (J1745−2820) relative to the maser source are indicated in columns 4 and 5. Typical flux densities (S_ν) and LSR velocities of the maser spots used for the parallax measurement and of the background source are given in columns 6 and 7. To avoid potential confusion, we note that the listed Sgr B2M maser spot was the interferometer phase reference, whereas the listed Sgr B2N maser spot was not the phase reference.

For both Sgr B2M and Sgr B2N, we used the background source, J1745−2820, as a position reference for the parallax and proper motion measurements (see Figure 1). J1745−2820 is a well-studied extragalactic radio source (Bower et al. 2001) that has been used in previous VLBA astrometric observations of Sgr A* (Reid & Brunthaler 2004). Table 2 lists the positions of these sources. J1745−2820 is projected only 20′ west of the maser sources, making it a nearly ideal position reference as it is very close to our maser targets, thereby canceling most systematic errors by a factor of ≈0.006 (the angular separation in radians). This occurs because the dominant source of systematic error for VLBI astrometry usually is unmodeled (large scale) atmospheric propagation delays which increase with target–background source separation (Reid et al. 1999). Since J1745−2820 is offset predominantly in the east–west direction from Sgr B2, both sources sample similar source zenith angles, which further reduces the effects of unmodeled atmospheric delays (Honma et al. 2008).

We alternated between two 16 minutes observing blocks, one for Sgr B2M and the other for Sgr B2N; each block consisted of observations of a maser cluster and J1745−2820. Within a block, we switched sources every 40 s during the first two epochs and every 15 s (in order to better monitor and remove rapid atmospheric phase fluctuations) during the remaining 10 epochs. We used a strong H_2O maser spot as the interferometer phase-reference, because it was considerably stronger than the background source and could be detected on individual baselines in the available on-source time as short as 8 s.

We placed observations of strong sources near the beginning, middle and end of the observations in order to monitor delay and electronic phase differences among the IF bands. In practice, however, we found minimal drifts and used only a single scan on J1642+4938 for this calibration. We did not attempt bandpass calibration as the variation in phase across the VLBA bandpasses are typically $<5^\circ$ across the central 90% of the band, and the masers were observed near band center. We also placed ≈40 minute "geodetic-like" observing blocks before, near the middle, and after the rapid switching blocks in order to monitor and remove the effects of zenith atmospheric path-length errors in the VLBA correlator model (Reid et al. 2009a).

The rapid-switching observations employed four adjacent frequency bands of 8 MHz bandwidth and recorded both right and left circularly polarized signals. The four (dual-polarized) bands were centered at local standard of rest velocities ($v_{\rm LSR}$) of 158, 50, −58, and −166 km s^{-1} for both maser sources, with almost all known Sgr B2 maser signals contained in the second band (McGrath et al. 2004). The raw data were recorded on transportable disks at each antenna and shipped to the VLBA correlation facility in Socorro, NM. The data from individual antenna pairs were cross-correlated with an integration time of 0.52 s. Integration times were kept short to allow position shifting of the data to accommodate a priori uncertainties in the maser positions. With this short integration time, we could not process all eight frequency bands in one pass with sufficient spectral resolution for the masers, without exceeding the maximum correlator output rate. Thus, we correlated the data in two passes. One pass was processed with 16 spectral channels for each of the eight frequency bands. These data were used for the geodetic blocks (to determine atmospheric delays and clock drifts) and for the background continuum sources observed in rapid-switching (phase-referencing) mode. Another pass was processed with 256 spectral channels, but only for the single (dual-polarized) frequency band containing the maser signals, giving spectral channels separated by 0.42 km s^{-1}, assuming a rest frequency of 22235.08 MHz for the $6_{16} \rightarrow 5_{23}$ transition of H_2O.

Calibration of the interferometer data was done with the Astronomical Image Processing System (AIPS) in a manner described by Reid et al. (2009a) for methanol maser parallaxes. A single spectral-channel of the maser data was used for the interferometer phase reference. For Sgr B2M, a maser spot at $v_{\rm LSR} = 66.4$ km s^{-1} served as the phase reference and was compact (≈ 0.3 mas FWHM) and detectable at all epochs with typical strength of 40 Jy. Test imaging of this spot showed a nearly unresolved source with high dynamic range (>100:1), indicating a clean reference source. When calculating reference phases it is important to have very low residual fringe rates in order to avoid degrading the image of the target source (Beasley & Conway 1995), in our case J1745−2820. Since the position of J1745−2820 was known to better than 10 mas accuracy (Reid & Brunthaler 2004), we could measure its *apparent* map offset when phase referenced to a maser spot and correct the position of the maser (to better than 10 mas accuracy) before final processing. For the Sgr B2M reference spot this required a position shift of $(\Delta\alpha \cos\delta, \Delta\delta) = (1\farcs594, -1\farcs399)$; the same shift was used for all 12 epochs, canceling to second order the effects associated with the error in this shift. (This shift should be added to the correlation coordinates in Table 2 to give the true position of the reference maser spot.)

For Sgr B2N, no strong maser spot suitable as a phase reference was found to persist for all 12 epochs. Therefore, we used the maser spot at $v_{\rm LSR} = 52.5$ km s^{-1} as the reference for epochs A through I, over which time it displayed $S_\nu > 20$ Jy. For epochs K through N the spot at $v_{\rm LSR} = 38.6$ km s^{-1} was used as the reference over which time it displayed $S_\nu > 180$ Jy. As described above, we determined position shifts relative to the coordinates used for correlation (Table 2) for these two reference spots, based on trial calibration and imaging of J1745−2820. The spot at $v_{\rm LSR} = 52.5$ km s^{-1} was found at $(\Delta\alpha \cos\delta, \Delta\delta) = (0\farcs023, 0\farcs028)$ and the spot at $v_{\rm LSR} = 38.6$ km s^{-1} at $(\Delta\alpha \cos\delta, \Delta\delta) = (-0\farcs011, 0\farcs006)$. The effects of these shifts were removed from the maser data for epochs A through I and from epochs K through N, respectively, before determining reference phases.

Reference phases were interpolated from those measured at the times of the maser observations to the times of the J1745−2820 observations and subtracted from all data. Phase reference data for each baseline were examined for jumps greater than 60° between adjacent maser scans and, when found, the J1745−2820 data between these scans were discarded. Calibrated data for J1745−2820 were imaged with the AIPS task IMAGR. All data with source elevation less than 20° were discarded, owing to greatly increased sensitivity to atmospheric delay errors compared to higher elevation data. While interferometer fringes were obtained on the longest baselines for the maser data, indicating maser spot sizes of ≈0.3 mas, the background continuum source was considerably larger, probably owing to scatter broadening (Bower et al. 2001), and we could only effectively image this source with baselines shorter than 1500 km. Unfortunately, this reduced our astrometric accuracy by a factor of ≈4 compared to the Sgr B2 masers which could be detected on the longest VLBA baselines. For J1745−2820 we used a (u, v)-cellsize of 0.1 mas and a CLEAN Gaussian restoring beam with a FWHM of 1.5 mas. Images were fitted with a single elliptical Gaussian model using the task JMFIT.

3. RESULTS

Parallax data was obtained by subtracting the apparent position of J1745−2820 from those of a maser spot that could be detected at all epochs. For Sgr B2M we used the phase-reference spot for the parallax measurement. However, for Sgr B2N, neither phase-reference spot persisted for the entire year and we selected different maser spots for the parallax measurement. When analyzing this data, we corrected for the difference in the shifts used for the two different reference maser spots. The measured position differences are given in Table 3.

Formal position fitting uncertainties are quite small (generally <0.02 mas toward the east and <0.04 mas toward the north) for both the strong maser spots and J1745−2820 observed with the VLBA. However, realistic uncertainties need to account for systematic effects, usually dominated by residual errors in (mostly tropospheric) propagation delays after calibration, and possibly structural changes in the maser spots and/or in the

Table 3
VLBA Position Measurements

Source	v_{LSR} (km s^{-1})	Epoch (yr)	Δx (mas)	Δy (mas)
Sgr B2M...	66.4	2006.676	$+0.318 \pm 0.050$	$+2.076 \pm 0.150$
		2006.728	$+0.255 \pm 0.050$	$+2.131 \pm 0.150$
		2006.772	$+0.222 \pm 0.050$	$+1.665 \pm 0.150$
		2006.813	$+0.260 \pm 0.050$	$+2.046 \pm 0.150$
		2007.189	-0.025 ± 0.025	$+0.241 \pm 0.075$
		2007.208	-0.048 ± 0.025	$+0.240 \pm 0.075$
		2007.230	-0.120 ± 0.025	$+0.117 \pm 0.075$
		2007.287	-0.151 ± 0.025	-0.169 ± 0.075
		2007.307	-0.183 ± 0.025	-0.174 ± 0.075
		2007.742	-1.051 ± 0.050	-1.921 ± 0.150
		2007.747	-0.944 ± 0.050	-1.873 ± 0.150
		2007.791	-0.975 ± 0.050	-1.967 ± 0.150
Sgr B2N...	56.7	2006.676	193.960 ± 0.060	-33.656 ± 0.140
		2006.728	193.689 ± 0.060	-34.273 ± 0.140
		2006.772	193.775 ± 0.060	-34.213 ± 0.140
		2006.813	193.634 ± 0.060	-34.833 ± 0.140
		2007.189	193.804 ± 0.030	-36.506 ± 0.070
		2007.208	193.835 ± 0.030	-36.532 ± 0.070
		2007.230	193.751 ± 0.030	-36.712 ± 0.070
		2007.287	193.796 ± 0.030	-36.979 ± 0.070
		2007.307	193.747 ± 0.030	-37.007 ± 0.070
		2007.742	193.340 ± 0.060	-39.090 ± 0.140
		2007.747	193.420 ± 0.060	-38.917 ± 0.140
		2007.791	193.381 ± 0.060	-39.240 ± 0.140

Notes. Data used for parallax and proper motion fits for an H_2O maser spot in Sgr B2M and Sgr B2N. Columns 4 and 5 are position differences between the maser spot and a compact extragalactic source J1745−2820, relative to the coordinates used to correlate the VLBA data and any shifts applied in calibration (see Section 2); position differences are in the eastward ($\Delta x = \Delta\alpha \cos\delta$) and northward directions ($\Delta y = \Delta\delta$). The large offsets for the Sgr B2N maser spot reflect its position relative to the adopted phase reference at $v_{LSR} = 52.5$ km s^{-1}.

background source. Also, the typically phase-stable weather for early morning observations in late winter/early spring produced significantly better phase reference data than the late evening observations in late summer/early fall. We estimated realistic uncertainties from the quality of the phase reference data as well as the scatter among positions measured at closely spaced epochs. These uncertainties are listed in Table 3 and were used to weight the data when fitting for parallax and proper motion.

The model for the data consisted of the sum of the sinusoidal parallax signature (corrected for the eccentricity of the Earth's orbit about the Sun) and a linear proper motion in each coordinate. We performed least-squares fits separately for the Sgr B2M and Sgr B2N data. Table 4 and Figures 2 and 3 show the parallax and proper motion fitting results for the Sgr B2M and Sgr B2N H_2O masers.

The Sgr B2M data for the maser spot at $v_{LSR} = 66.4$ km s^{-1} could be well fitted by the model with a parallax of 0.130 ± 0.012 mas and a post-fit chi-squared per degree of freedom $\left(\chi^2_{pdf}\right)$ near unity. At two epochs one of the important "inner-5" VLBA antennas was not available (OV at 2007 March 25 = 2007.230 and FD at 2007 September 28 = 2007.742) and the post-fit residuals were somewhat larger than most others. Removing these points resulted in a parallax of 0.127 ± 0.012 mas, which is very close to the parallax using all data; we adopted the fit using all data. We also tested the sensitivity of the parallax to the errors assigned to the data by assuming uniform values for each coordinate. We achieved a χ^2_{pdf} of unity for errors of 0.037 mas and 0.143 mas for the eastward and northward data and a parallax of 0.132 ± 0.013 mas. Thus, details of weighting the data had little effect on the parallax measurement.

The Sgr B2N data for the maser spot at $v_{LSR} = 56.7$ km s^{-1} displayed a bit more scatter than the Sgr B2M data. Using all data, the parallax for Sgr B2N was 0.111 ± 0.019 mas. The first epoch point appeared discrepant and after removing it the fit improved considerably, yielding a parallax of 0.128 ± 0.015 mas. We adopt this result for Sgr B2N. Some other maser spots (spectral channels at $v_{LSR} = 47.9$, 47.5, 47.1, 42.0, and 41.6 km s^{-1}) could be detected at all epochs and yielded nearly identical parallaxes. However, comparison of the post-fit residuals indicated that the data from different spectral channels were highly correlated, and thus combining the results from these channels produces no significant improvement for the parallax result. This does, however, indicate that potential variations of the maser spot structure is not an important source of systematic uncertainty.

Since the Sgr B2M and Sgr B2N data were taken at different times (interleaved observations; see Section 2) and are *statistically* independent, one could consider combining the solutions and obtaining some improvement in parallax accuracy. However, a detailed comparison of the data suggests that systematic errors common to both sources are significant. One can see, in the right-hand panels of Figures 2 and 3, similar deviations in post-fit residuals (departures from the fitted line) for the two maser sources for the five epochs in early 2007 and the three epochs in late 2007. But, the residuals for the four epochs in late 2006 show no strong correlation, suggesting that the results for the two maser sources are not entirely correlated. However, we will be conservative when quoting a single parallax for the Sgr B2 region and not reduce the uncertainty when averaging the parallaxes from the two sources. Thus, our combined result is that Sgr B2 region has a parallax of 0.129 ± 0.012 mas, corresponding to a distance of $7.8^{+0.8}_{-0.7}$ kpc.

Table 4
Parallaxes & Proper Motions for Sgr B2

Source	ℓ (deg)	b (deg)	Parallax (mas)	μ_x (mas yr^{-1})	μ_y (mas yr^{-1})	v_{LSR} (km s^{-1})
Sgr B2N...	0.677	−0.028	0.128 ± 0.015	-0.32 ± 0.05	-4.69 ± 0.11	64 ± 5
Sgr B2M...	0.667	−0.035	0.130 ± 0.012	-1.23 ± 0.04	-3.84 ± 0.11	61 ± 5

Notes. Parallax and proper motion fits using the data in Table 3. Columns 2 and 3 give Galactic longitude and latitude, respectively. Columns 4, 5 and 6 list the parallax and proper motions in the eastward ($\mu_x = \mu_\alpha \cos\delta$) and northward directions ($\mu_y = \mu_\delta$), respectively. Column 7 lists the central local standard of rest velocity of dense molecular gas associated with the maser sources (Reid et al. 1988; Sutton et al. 1991).

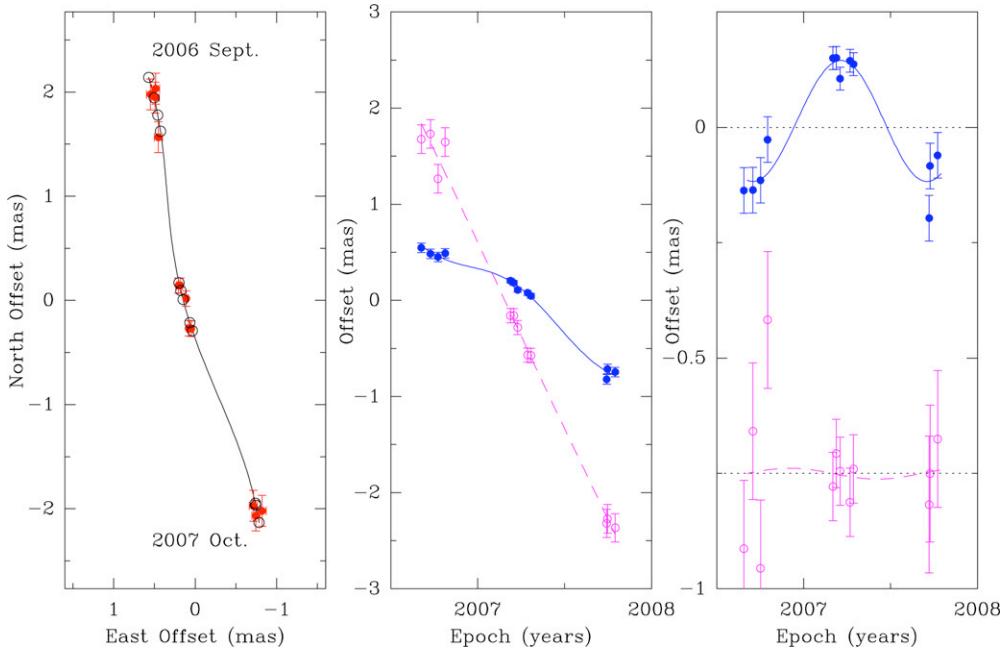

Figure 2. Parallax and proper motion data and fits for Sgr B2M. Plotted are position measurements of an H_2O maser spot at $v_{LSR} = 66.4$ km s^{-1} relative to the background source J1745−2820. Left panel: positions on the sky (red circles) with first and last epochs labeled. The expected positions from the parallax and proper motion fit are indicated (black circles and solid line). Middle panel: east (filled blue circles and solid line) and north (open magenta circles and dashed line) position offsets and best fit parallax and proper motions fit versus time. The northward data have been offset from the eastward data for clarity. Right panel: same as the middle panel, except the best fit proper motion has been removed, allowing the effects of only the parallax to be seen.

(A color version of this figure is available in the online journal.)

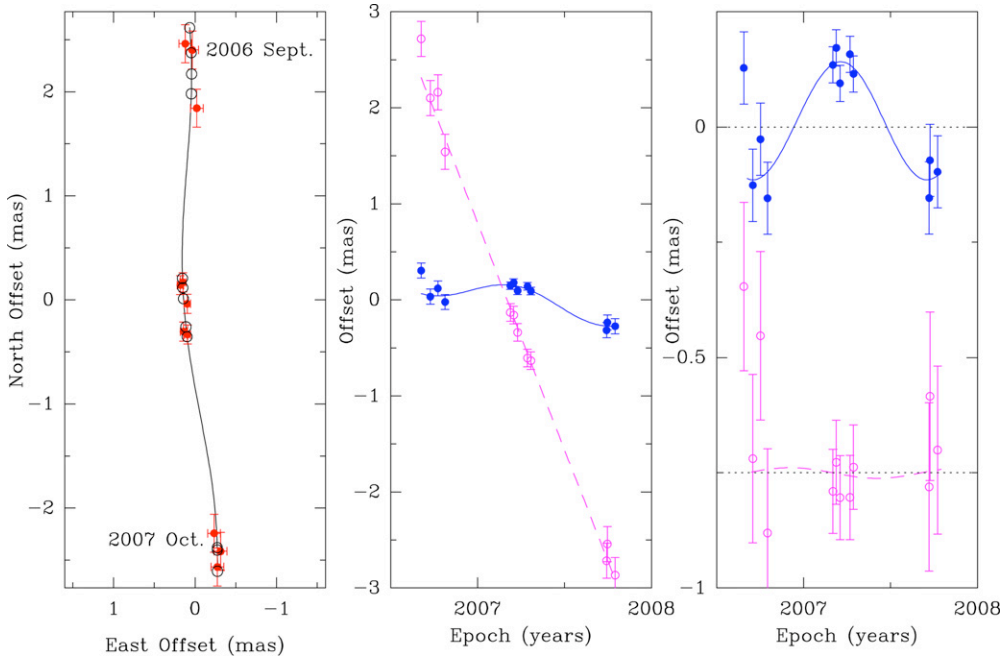

Figure 3. Parallax and proper motion data and fits for Sgr B2N. Plotted are position measurements of an H_2O maser spot at $v_{LSR} = 56.7$ km s^{-1} relative to the background source J1745−2820. Left panel: positions on the sky (red circles) with first and last epochs labeled. The expected positions from the parallax and proper motion fit are indicated (black circles and solid line). The first epoch point appears to be an outlier and was not used for the fitting. Middle panel: east (filled blue circles and solid line) and north (open magenta circles and dashed line) position offsets and best fit parallax and proper motions fit versus time. The northward data have been offset from the eastward data for clarity. Right panel: same as the middle panel, except the best fit proper motion has been removed, allowing the effects of only the parallax to be seen.

(A color version of this figure is available in the online journal.)

4. DISCUSSION

Our measurement of the distance to Sgr B2 almost certainly can be taken as a measure of R_0, the Galactic center distance. Evidence that Sgr B2 is very close to the Galactic center (i.e., SgrA) has been summarized by Reid et al. (1988), and includes the following observations. (1) Sgr B2 is a nearly unique source with the greatest variety of detected molecular species of any molecular cloud, owing to the high densities near the Galactic center (Snyder et al. 1994; Belloche et al. 2008). (2) It is

projected ≈0.09 kpc from the Galactic center, which suggests an expected line-of-sight component of 0.07 kpc. (3) Atomic and molecular absorption studies locate Sgr B2 within the "270-pc expanding shell" (Scoville 1972).

Since we have also measured the proper motions of maser spots in Sgr B2, we can estimate its three-dimensional location, provided it is on a nearly circular Galactic orbit. For an object near the Galactic center on a low eccentricity orbit in the plane, the distance offset along the line of sight from the center, d, is given by $d = r_{\rm proj} R_0 \mu_{\rm Gal}/v_{\rm LSR}$, where $r_{\rm proj}$ is the projected distance on the sky and $\mu_{\rm Gal}$ is the proper motion in Galactic longitude in a reference frame not rotating with the Galaxy. Our measured proper motions for a small number of maser spots in Sgr B2M and Sgr B2N gives an average motion in Galactic longitude of -4.05 mas yr^{-1}, with a probable uncertainty of about 1 mas yr^{-1} because we have not accounted for internal motions in the two H_2O maser sources. (A complete mapping of the ∼100 maser spots in each source for multiple epochs is beyond the scope of this paper and will be published later.) Subtracting the apparent motion of Sgr A* of -6.379 mas yr^{-1} in Galactic longitude (Reid & Brunthaler 2004; in order to correct for the apparent motion expected from the solar orbit) yields a true motion in the direction of increasing Galactic longitude of $\mu_{\rm Gal} \approx 2.3 \pm 1.0$ mas yr^{-1}. Adopting $R_0 \approx 8$ kpc and $v_{\rm LSR} \approx 62$ km s^{-1}, this suggests $d \approx 0.13 \pm 0.06$ kpc. This estimate of the offset of Sgr B2 from Sgr A* rests on the assumption of a low eccentricity Galactic orbit for Sgr B2. This assumption might be testable in the future when the full space motion of Sgr B2 is accurately measured and the gravitational potential in the Galactic center region is better known. However, since the offset of Sgr B2 from Sgr A* is almost certainly much smaller than our (current) distance measurement uncertainty, the exact value of the offset is probably of little significance.

Correcting for the small estimated offset of Sgr B2 relative to Sgr A* of 0.13 kpc (with Sgr B2 closer than Sgr A*), we find $R_0 = 7.9^{+0.8}_{-0.7}$ kpc. While this estimate of R_0 is not (yet) as accurate as, for example, that obtained from stellar orbits in the Galactic center, a trigonometric parallax is the "gold standard" for distances and provides improved confidence in any estimate of R_0. The uncertainty in R_0 can be reduced by continued observations (with $\sigma_{R_0} = 1/\sqrt{N}$ for N similar yearly observations). Improved accuracy could also come from the discovery of another suitable extragalactic reference source that is less scatter broadened than J1745−2820.

X.W.Z. and Y.X. were supported by the Chinese National Science Foundation, through grants NSF 10673024, 10733030, 10703010 and 10621303, and by the NBPRC (973 Program) under grant 2007CB815403.

Facilities:VLBA

REFERENCES

Beasley, A. J., & Conway, J. E. 1995, in ASP Conf. Ser. 82, Very Long Baseline Interferometry and the VLBANRAO, ed. J. A. Zensus, P. J. Diamond, & P. J. Napier (San Francisco, CA: ASP), 328
Belloche, A., et al. 2008, A&A, 482, 179
Bica, E., Bonatto, c., Barbuy, B., & Ortolani, S. 2006, A&A, 450, 105
Bower, G. C., Backer, D. C., & Sramek, R. A. 2001, ApJ, 558, 127
Damour, T., & Taylor, J. H. 1991, ApJ, 366, 501
Elmegreen, B. G., Genzel, R., Moran, J. M., Reid, M. J., & Walker, R. C. 1980, ApJ, 241, 1007
Freedman, W. L., et al. 2001, ApJ, 553, 47
Ghez, A. M., et al. 2008, ApJ, 689, 1044
Gillessen, S., Eisenhauer, F., Trippe, S., Alexander, T., Genzel, R., Martins, F., & Ott, T. 2009, ApJ, 692, 1075
Hachisuka, K., Brunthaler, A., Menten, K. M., Reid, M. J., Hagiwara, Y., & Mochizuki, N. 2009, ApJ, 696, 1981
Herrnstein, J. R., et al. 1999, Nature, 400, 539
Honma, M., Tamura, Y., & Reid, M. J. 2008, PASJ, 60, 951
Honma, M., et al. 2007, PASJ, 59, 889
LaRosa, T. N., Kassim, N. E., Lazio, T. J. W., & Hyman, S. D. 2000, AJ, 119, 207
Macri, L. M., Stanek, K. Z., Bersier, D., Greenhill, L. J., & Reid, M. J. 2006, ApJ, 652, 1133
McGrath, E. J., Goss, W. M., & De Pree, C. G. 2004, ApJ, 155, 577
Oort, J. H., & Plaut, L. 1975, A&A, 41, 71
Reid, M. J. 1993, ARA&A, 31, 345
Reid, M. J., & Brunthaler, A. 2004, ApJ, 616, 872
Reid, M. J., Menten, K. M., Brunthaler, A., Zheng, X. W., Moscadelli, L., & Xu, Y. 2009a, ApJ, 693, 397
Reid, M. J., Readhead, A. C. S., Vermeulen, R. C., & Treuhaft, R. N. 1999, ApJ, 524, 816
Reid, M. J., Schneps, M. H., Moran, J. M., Gwinn, C. R., Genzel, R., Downes, D., & Roennaeng, B. 1988, ApJ, 330, 809
Reid, M. J., et al. 2009b, ApJ, 700, 137
Scoville, N. 1972, ApJ, 175, L127
Shapley, H. 1918, ApJ, 48, 154
Shattow, G., & Loeb, A. 2008, MNRAS, 392, L21
Snyder, L. E., Kuan, Y.-J., & Miao, Y. 1994, in Lecture Notes in Physics 439, The Structure and Content of Molecular Clouds, ed. T. L. Wilson & K. J. Johnston (Berlin: Springer), 187
Sutton, E. C., Jaminet, P. A., Danchi, W. C., & Blake, G. A. 1991, ApJS, 77, 255
Trimble, V. 1986, Comments Astrophys., 11, 257
Vanhollebeke, E., Groenewegen, M. A. T., & Girardi, L. 2009, A&A, 498, 95
Xu, Y., Reid, M. J., Zheng, W. W., & Menten, K. M. 2006, Science, 311, 54